Pergamon

Int. J. Heat Mass Transfer. Vol. 40, No. 8, pp. 1825–1834, 1997

0017–9310/97 $17.00+0.00

PII: S0017–9310(96)00255–4

Numerical prediction of lock-on effect on convective heat transfer from a transversely oscillating circular cylinder

CHIN-HSIANG CHENG, JING-LIA HONG

Department of Mechanical Engineering, Tatung Institute of Technology, Taipei, Taiwan, Republic of China

and

WIN AUNG†

Division of Engineering Education and Centers, National Science Foundation, Arlington, Virginia, U.S.A.

(*Received* 7 *November* 1995 *and in final form* 1 *July* 1996)

Abstract—Heat transfer characteristics and the flow behavior of cross flow over a transversely oscillating cylinder are investigated. The lock-on phenomenon has been predicted numerically and its influence on the heat transfer performance of the cylinder is evaluated. The SOLA method is employed to solve the unsteady velocity field in a non-inertial reference frame, and the energy equation is solved by a finite-volume method. Transient variations of the Nusselt number and the drag and lift coefficients are calculated for various oscillation conditions. The ranges of the dominant parameters considered in this study are $0 \leqslant Re \leqslant 300$, $0 \leqslant S_c \leqslant 0.3$ and $0 \leqslant A/D \leqslant 0.7$. The Prandtl number is considered to be 0.71 or 7.0. In the lock-on regime, an appreciable heat transfer increase caused by the oscillation is observed; however, outside this regime, the heat transfer is almost unaffected by the oscillation. A correlation formula expressing the dependence of heat transfer on these dominant parameters in this lock-on regime is presented. The numerical predictions have been compared with the existing information, and good agreement has been found.

INTRODUCTION

The convective heat transfer from a stationary circular cylinder has been extensively studied. The applications range from hot-wire anemometers to nuclear reactors. It is recognized that the Reynolds number is a dominant parameter governing the flow pattern and the heat transfer characteristics. Periodic drag and lift forces exerted on the cylinder, which accompany the periodic vortex shedding in the wake behind the cylinder, can be observed at Reynolds numbers higher than about 50 [1–11]. The predominant frequency of vortex shedding has been measured and referred to as the natural shedding frequency (f). The Strouhal number, defined by fD/u_0, represents the dimensionless natural shedding frequency and is essentially a function of the Reynolds number. The unsteady flow close to the cylinder surface causes unsteady heat transfer on the cylinder. Previous numerical analyses and experimental studies have shown that the temperature field changes periodically at the same frequency and that the maximum local heat transfer rate may be found in the area near the stagnation point [11–21].

As the cylinder is forced to oscillate transversely in the direction normal to the flow stream, a nonlinear interaction occurs particularly as the cylinder oscillation frequency (s_c) gradually approaches the natural frequency of vortex shedding (f). This interaction leads to two major flow phenomena. First, in the wake, the frequency of vortex shedding suddenly shifts from the natural frequency to the cylinder oscillation frequency. A resonance between the vortex shedding and the cylinder oscillation is maintained over a range of oscillation frequency. As the oscillation frequency of the cylinder is elevated to a threshold value, the frequency of vortex shedding changes to the natural frequency again and is independent of the oscillation of the cylinder. Secondly, the drag force is appreciably increased to attain a peak value at the mid-point of the resonance regime. This regime is termed the 'lock-on' or 'wake capture' regime that has been studied by many authors [22–25].

Considering the effect of the oscillation of the cylinder on forced convection, Kezios and Prasanna [26] reported a 20% increase in the average heat transfer coefficient from a transversely oscillating cylinder.

† Adjunct Professor, College of Engineering, Southern Illinois University, Carbondale, IL, U.S.A.

NOMENCLATURE

A	amplitude of oscillation of cylinder
C_d	drag coefficient, equation (12)
$\overline{C_d}$	time-averaged drag coefficient, equation (17a)
$\overline{C_{dPL}}$	peak value of time-averaged drag coefficient in the lock-on regime
C_L	life coefficient, equation (13)
D	cylinder diameter
f	natural shedding frequency
Nu	overall Nusselt number, equation (16)
Nu_θ	local Nusselt number, equation (14)
$\overline{Nu}$	time-averaged overall Nusselt number, equation (17b)
$\overline{Nu_{PL}}$	peak value of time-averaged overall Nusselt number in lock-on regime
$\overline{Nu_0}$	time-averaged overall Nusselt number for stationary cylinders
$\overline{Nu_\theta}$	time-averaged local Nusselt number, equation (15)
p	pressure
p_∞	pressure at far field
P	dimensionless pressure
Pr	Prandtl number
r, θ	cylindrical coordinates
R, θ	dimensionless cylindrical coordinates
Re	Reynolds number, $u_0 D/\nu$
s_c	frequency of oscillation of cylinder
S_c	dimensionless frequency of oscillation of cylinder, $s_c D/u_0$
S_{c0}	dimensionless natural shedding frequency or dimensionless oscillation frequency at the peak of lock-on regime
St	Strouhal number or dimensionless natural shedding frequency, fD/u_0
$\bar{t}$	time
t	dimensionless time
t_p	dimensionless cycle period of oscillation of cylinder
t_0	arbitrary time start
T	temperature
T_w	wall temperature
T_∞	temperature at far field
$\bar{T}$	dimensionless temperature
u	velocity component in r-direction
u_0	free stream velocity
U	dimensionless velocity component in R-direction
v	velocity component in θ-direction
V	dimensionless velocity component in θ-direction.

Greek symbols

α_f	thermal diffusivity of fluid
ν	kinematic viscosity
ρ	fluid density.

Saxena and Laird [27] considered a 22 mm diameter cylinder transversely oscillating in an open water channel for a flow at $Re = 3500$ and observed a 60% increase in heat transfer. However, in an earlier study by Sreenivasan and Ramachandran [28], no appreciable change in the heat transfer coefficient was found to accompany cylinder oscillation in air flow. Leung, Ko and Ma [29] found that for $Re < 15000$, the heat transfer may be enhanced as either the oscillation frequency or amplitude is increased; however, the oscillation effect becomes weaker as the Reynolds number is increased. Recently, Cheng, Chen, and Aung [30] performed an experimental study for flows with $0 \leqslant S_c \leqslant 0.65$, $0 \leqslant A/D \leqslant 0.628$ and $0 \leqslant Re \leqslant 4000$. According to their experimental data, the lock-on and the turbulence effects are two major mechanisms that could significantly enhance the forced convection. A maximum 34% increase in heat transfer was reached when the flow became turbulent; however, for a cylinder oscillating in a laminar cross flow, the increase in heat transfer coefficient was found only in the lock-on regime, and a 16% increase due to the lock-on effect was observed. In ref. [30], the lock-on phenomenon was also observed by flow visualization technique.

Numerical analyses, although restricted to laminar flows at low Reynolds numbers, offer another valuable tool to understanding the structure of the oscillation-influenced flow fields and provide insight not easily obtainable with experimental techniques. So far, however, almost all the previous numerical studies have been conducted to evaluate the effects of oscillation on the flow fields [9, 23, 24]. Only a few reports deal with the heat transfer problem. As a result, the theoretical information on the oscillation-enhanced heat transfer is still insufficient. The numerical approach becomes necessary to provide further understanding and to clarify some inconsistency in the experimental data reported by the various authors [26–30]. Before the conclusion of the present study, a numerical work presented by Karanth, Rankin, and Sridhar [31] comes to our attention. These authors provide the data for the flow over a transversely oscillating cylinder that exactly lies within the lock-on regime at $Re = 200$, which are seemingly the only available numerical solutions for the heat transfer behavior of an oscillating cylinder. However, in their study, the Reynolds number is limited at 200 and the cylinder is considered to oscillate exactly at a fixed lock-on frequency. The solution at other Reynolds number is

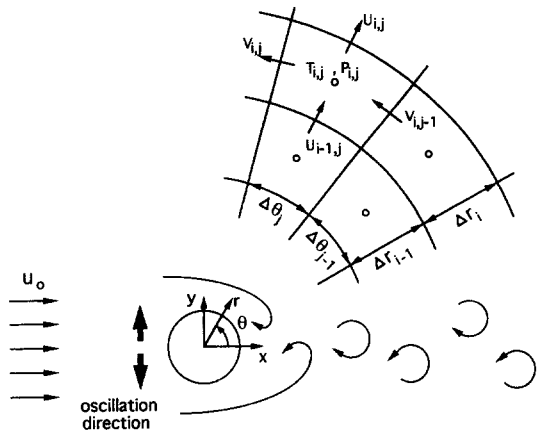

Fig. 1. An oscillating cylinder in a uniform flow.

not available, and the difference between the lock-on and the unlock-on flows has not been discussed. To have a deeper insight into the lock-on behavior, a more general study is definitely necessary.

The purpose of the present study is to develop a theoretical model for numerical predictions of convective heat transfer on an oscillating cylinder for various oscillation conditions and Reynolds numbers. The lock-on and unlock-on phenomena are predicted numerically. The influence of the lock-on effects on the heat transfer performance of the cylinder is also evaluated to verify the experimental data previously obtained by Cheng, Chen and Aung [30].

The SOLA method proposed by Hirt, Nichols and Romero [32] is modified and adopted to solve the unsteady velocity field in a non-inertial reference frame. The energy equation is solved for the solutions of temperature distribution by a finite-volume method similar to that employed by Cheng, Luy and Huang [33].

The physical model of the present problem is shown in Fig. 1. A circular cylinder of diameter D is maintained at a uniform temperature T_w and is oscillating transversely in a uniform fluid stream. The vortices shed downstream in the wake of the cylinder are indicated. Also shown is the grid system for numerical computation. Four major parameters are considered in the analysis. The Reynolds number ranges from 0 to 300. The second parameter is the dimensionless frequency of the oscillation of the cylinder ($S_c = s_c D/u_0$) which is varied in the range $0 \leqslant S_c \leqslant 0.3$. The third parameter, the dimensionless oscillation amplitude (A/D), is in the range $0 \leqslant A/D \leqslant 0.7$. In addition, the Prandtl number is assigned to be 0.71 or 7.0.

THEORETICAL ANALYSIS

The properties of the fluid are assumed constant, and the buoyancy force is assumed to be relatively small compared with the inertial force. The non-inertial reference frame moves with the oscillating cylinder with

$$y = A\sin(2\pi s_c \bar{t}). \tag{1}$$

In the cylindrical coordinate on a non-inertial reference frame, the dimensionless governing equations for a laminar flow are expressed as:

$$\frac{U}{R} + \frac{\partial U}{\partial R} + \frac{1}{R}\frac{\partial V}{\partial \theta} = 0 \tag{2}$$

$$\frac{\partial U}{\partial t} + \frac{\partial U^2}{\partial R} + \frac{1}{R}\frac{\partial UV}{\partial \theta} + \frac{U^2}{R} - \frac{V^2}{R} = -\frac{\partial P}{\partial R} + \frac{1}{Re}\left(\frac{\partial^2 U}{\partial R^2} + \frac{1}{R}\frac{\partial U}{\partial R} - \frac{U}{R^2} + \frac{1}{R^2}\frac{\partial^2 U}{\partial \theta^2} - \frac{2}{R^2}\frac{\partial V}{\partial \theta}\right) + 4\pi^2 S_c^2 \bar{A}\sin(2\pi S_c t)\sin\theta \tag{3}$$

$$\frac{\partial V}{\partial t} + \frac{\partial UV}{\partial R} + \frac{1}{R}\frac{\partial V^2}{\partial \theta} + \frac{2UV}{R} = -\frac{1}{R}\frac{\partial P}{\partial \theta} + \frac{1}{Re}\left(\frac{\partial^2 V}{\partial R^2} + \frac{1}{R}\frac{\partial V}{\partial R} - \frac{V}{R^2} + \frac{1}{R^2}\frac{\partial^2 V}{\partial \theta^2} + \frac{2}{R^2}\frac{\partial U}{\partial \theta}\right) + 4\pi^2 S_c^2 \bar{A}\sin(2\pi S_c t)\cos\theta \tag{4}$$

$$\frac{\partial \bar{T}}{\partial t} + U\frac{\partial \bar{T}}{\partial R} + \frac{V}{R}\frac{\partial \bar{T}}{\partial \theta} = \frac{1}{Pr\,Re}\left(\frac{1}{R}\frac{\partial \bar{T}}{\partial R} + \frac{\partial^2 \bar{T}}{\partial R^2} + \frac{1}{R^2}\frac{\partial^2 \bar{T}}{\partial \theta^2}\right). \tag{5}$$

The dimensionless parameters are defined by

$$R = \frac{r}{D} \quad t = \frac{\bar{t}u_0}{D} \quad U = \frac{u}{u_0} \quad V = \frac{v}{u_0} \quad P = \frac{p - p_\infty}{\rho u_0^2}$$

$$\bar{T} = \frac{T - T_\infty}{T_w - T_\infty} \quad Pr = \frac{\nu}{\alpha_f} \quad Sc = \frac{s_c D}{u_0} \quad Re = \frac{u_0 D}{\nu} \quad \bar{A} = \frac{A}{D}$$

where s_c and A represent the frequency and the amplitude of the oscillation of the cylinder, respectively. Note that the velocity components in r- and θ-directions, u and v, are actually the velocity components relative to the cylinder. The reference frame transformation produces two acceleration terms, $4\pi^2 S_c^2 \bar{A}\sin(2\pi S_c t)\sin\theta$ and $4\pi^2 S_c^2 \bar{A}\sin(2\pi S_c t)\cos\theta$, in equations (3) and (4), respectively.

Boundary conditions

As a result of the reference frame transformations, a no-slip boundary condition and an oscillating fluid stream are specified on the cylinder surface. The no-slip and the isothermal conditions on the surface of the cylinder are given as

$$U = 0, V = 0, \quad \text{and} \quad \bar{T} = 1, \quad \text{at } R = 1/2. \tag{6}$$

At the far field, the boundary conditions are pre-

scribed by a potential flow solution with superimposed oscillating motion. That is, at $R \to \infty$,

$$U = (\cos\theta + 2\pi S_c \bar{A} \cos(2\pi S_c t) \sin\theta)\left(1 - \frac{1}{4R^2}\right) \tag{7a}$$

$$V = (-\sin\theta + 2\pi S_c \bar{A} \cos(2\pi S_c t) \cos\theta)\left(1 + \frac{1}{4R^2}\right) \tag{7b}$$

and

$$\bar{T} = 0. \tag{7c}$$

NUMERICAL METHODS

The SOLA method [32] is adopted in this study for efficiently dealing with the unsteady velocity fields. A staggered grid system shown in Fig. 1 is employed in the computation. The grid nodes for the pressure and other scalar quantities are placed at the centers of the cells, whereas those for the velocity components are located at the boundaries of the cells.

For each time step, the momentum equations are solved explicitly for a tentative velocity field. The tentative velocity components will not, in general, satisfy the continuity equation. These velocities are successively recalculated based on a relaxation of the pressure field until the continuity equation is satisfied at each cell. The computation proceeds to the next time level when the convergence of the adjustment is achieved. Detailed information for the iterative adjustment in the pressure and the velocity is available in ref. [32].

The finite difference form of the energy equation is derived by applying the control-volume integration to the equation over discrete cells, as described by Cheng, Luy and Huang [33]. The power-law scheme, recommended by Patankar [34], is used to handle the convective terms.

In addition, the present analysis uses a logarithmically spaced radial grid system which provides a finer grid size near the cylinder surface and a coarser grid at the far field. That is

$$R_i = R_{i-1} + e^{((i-2)/23.7 - 3.396)} \tag{8}$$

where i is the index grid point in the R-direction. The distance from the cylinder surface to the far edge of the solution domain is longer than fifty times cylinder diameter. Typically, a grid system of 100×100 grid points is employed in the analysis. The computation starts from the initially guessed velocity and temperature fields and is terminated when a periodically stable solution is attained.

RESULTS AND DISCUSSION

The solutions of velocity and temperature distributions enable the drag and lift coefficients and the Nusselt number to be further evaluated. The drag and lift coefficients are calculated by the equations

$$C_d = -\int_0^{2\pi} P|_{R=1/2} \cos\theta \, d\theta - \frac{1}{Re}\int_0^{2\pi} \left.\frac{\partial V}{\partial R}\right|_{R=1/2} \sin\theta \, d\theta \tag{9}$$

and

$$C_L = -\int_0^{2\pi} P|_{R=1/2} \sin\theta \, d\theta + \frac{1}{Re}\int_0^{2\pi} \left.\frac{\partial V}{\partial R}\right|_{R=1/2} \cos\theta \, d\theta \tag{10}$$

respectively.

The local Nusselt number around the cylinder surface is defined by

$$Nu_\theta(\theta, t) = \frac{-D}{T_w - T_\infty}\frac{\partial T}{\partial r} = -\left.\frac{\partial \bar{T}}{\partial R}\right|_{R=1/2}. \tag{11}$$

Integration of the local Nusselt number over one cycle of the oscillation of the cylinder leads to the time-averaged local Nusselt number

$$\overline{Nu_\theta}(\theta) = \frac{1}{t_p}\int_0^{t_p} Nu_\theta \, dt \tag{12}$$

where t_p is the period of the oscillation of the cylinder. On the other hand, the overall Nusselt number may be defined with the integration of Nu_θ around the cylinder surface as

$$Nu(t) = -\frac{1}{2\pi}\int_0^{2\pi} \left.\frac{\partial \bar{T}}{\partial R}\right|_{R=1/2} d\theta. \tag{13}$$

The time-averaged drag coefficient and the time-averaged overall Nusselt number may then be calculated with

$$\overline{C_d} = \frac{1}{t_p}\int_0^{t_p} C_d \, dt \tag{14a}$$

$$\overline{Nu} = \frac{1}{t_p}\int_0^{t_p} Nu \, dt \tag{14b}$$

respectively.

Stationary cylinders

Since the stationary-cylinder case has been investigated extensively [1–21], a comparison may be made between the present numerical data and the existing information for this special case to check the validity of the numerical schemes.

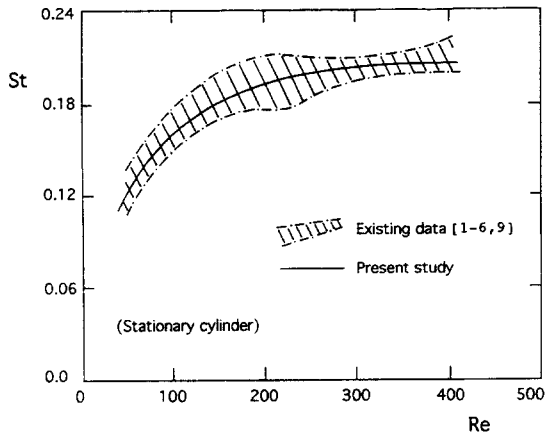

Fig. 2. Strouhal number as a function of Reynolds number for stationary-cylinder cases, compared with existing studies [1–6, 9].

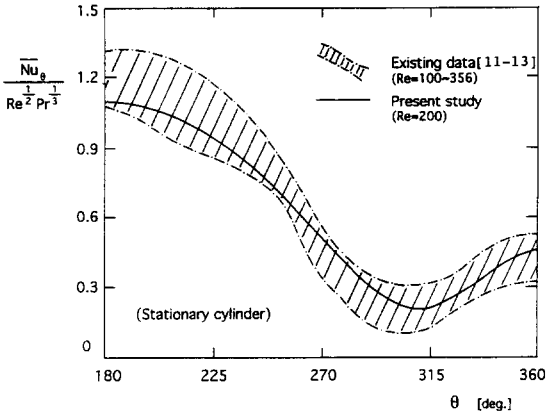

Fig. 3. Distribution of time-averaged local Nusselt number on the surface of a stationary cylinder at $Re = 200$, compared with existing studies [11–13].

Figure 2 shows the data of Strouhal number as a function of Reynolds number. The natural shedding frequency (f) can be detected directly from the periodically alternating velocity components at any points within the wake area. Some existing data [1–6, 9] are also given in this figure. It is observed that the present solution matches the existing data closely.

The time-averaged drag coefficient as a function of the Reynolds number for stationary cylinders is displayed in Table 1. The information from the previous studies [1–10], including experimental and numerical works, is reviewed and provided for comparison. Note that the existing data for the drag coefficient are somewhat scattered. Nevertheless, the predicted values are located within the ranges defined by the existing information.

Plotted in Fig. 3 is the distribution of the time-averaged local Nusselt number, in the form of $\overline{Nu_\theta}/Re^{1/2}Pr^{1/3}$, around the surface of a stationary cylinder at $Re = 200$. The shadowed area indicates the data from the previous studies [11–13]. The maximum local heat transfer rate is found at the front stagnation point ($\theta = 180°$). However, the vortex shedding downstream improves the local heat transfer on the rear face; therefore, a local peak value is found at $\theta = 360°$. Figure 4 shows the dependence of the time-averaged overall Nusselt number on the Reynolds number for the stationary-cylinder cases and at $Pr = 0.71$. Close agreement between the present numerical data and the existing information [12–21] may be observed.

Table 1. Time-averaged drag coefficient ($\overline{C_d}$) as a function of Reynolds number for stationary-cylinder cases, compared with existing studies [1–10]

Re	Ref. [1]	Ref. [2]	Ref. [3]	Ref. [4]	Ref. [5]	Ref. [6]	Ref. [7]	Ref. [8]	Ref. [9]	Ref. [10]	Present study
50	1.3818 | 1.450	—	—	—	—	—	—	—	—	1.405	1.40
80	—	—	—	—	1.235	—	1.270 | 1.280	—	—	—	1.33
100	1.24 | 1.2636	—	—	1.28	—	—	1.205 | 1.225	1.3618	—	1.2318	1.32
200	—	1.30	1.166 | 1.176	—	1.176	1.2665 | 1.2735	0.98 | 1.06	1.3818	1.25 | 1.33	1.1273	1.312
	Exp. 1959	Exp. 1960	Num. 1969	Num. 1972	Num. 1976	Num. 1979	Num. 1986	Num. 1986	Num. 1989	Num. 1991	Num.

Exp.—experimental study; Num.—numerical study.

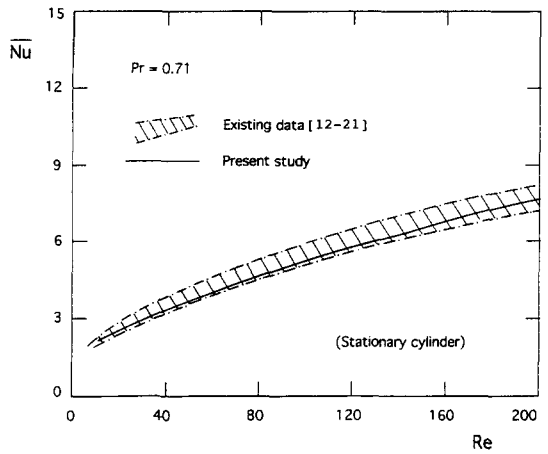

Fig. 4. Time-averaged overall Nusselt number as a function of Reynolds number for stationary-cylinder cases at $Pr = 0.71$, compared with existing studies [12–21].

Oscillating cylinders

To clearly display the predicted lock-on phenomenon, Fig. 5(a) and (b) is provided to show the flows located inside and outside the lock-on regime, respectively. At $Re = 80$, $Pr = 0.71$, and $A/D = 0.14$, two dimensionless frequencies of the oscillation of the cylinder, $S_c = 0.155$ and 0.3, are considered. The velocity and temperature fields are shown by means of the streamlines and the isotherms, respectively. Five plots showing the periodic variation of the velocity and temperature fields at five consecutive instants within one cycle of the oscillation of the cylinder are given in each of Fig. 5(a) and (b). Note that at $Re = 80$, the predicted Strouhal number is approximately 0.155. Therefore, by letting $S_c = 0.155$ in Fig. 5(a), the lock-on resonance is clearly observed. Notice that in Fig. 5(a) when the cylinder experiences one cycle, from $t = t_0$ to $t = t_0 + t_p$, and moves back to the starting position, the entire flow field also resumes its initial pattern. This implies that the vortices are shedding at a frequency exactly equal to the oscillation frequency of the cylinder. Also notice that the temperature field oscillates at the same frequency as the flow field.

When the value of S_c is elevated to 0.3, which is associated with an unlock-on flow, a rather different flow behavior is seen. As shown in Fig. 5(b), when the cylinder returns to the initial position after one cycle, the flow and temperature fields do not resume the initial state. The frequency of vortex shedding is now different from the frequency of the cylinder oscillation.

Numerical data for the increase of the time-averaged drag coefficient due to the lock-on effects are given in Fig. 6. Since the data at $Re = 80$ and $A/D = 0.14$ are available in the previous studies [22–24], a comparison for this particular case becomes possible. In this figure, an increase in drag coefficient is clearly observed in the lock-on regime. The calculations predict lower drag coefficient increase than that measured in the experiment of Tanida *et al.* [22]; however, the numerical results closely agree with the predicted values of Hurlbut *et al.* [23] and Chilukuri [24].

Figure 7 shows the lock-on effects by providing the time histories of overall Nusselt number and overall drag and life coefficients (Nu, C_d, and C_L) at $Re = 200$ and $Pr = 0.71$. The data of fluid temperature and velocity component in θ-direction ($\bar{T}$ and V) at point ($R = 5, \theta = 0$) are also given. The point ($R = 5, \theta = 0$) is located in the wake area. Figure 7(a) provides the predictions of these quantities for a stationary-cylinder case. Note that the natural shedding frequency is detected from the oscillating velocity data. The overall Nusselt number is found to be varying with a small amplitude at twice the natural shedding frequency, as was also discussed by Karanth, Rankin and Sridhar [31]. The life coefficient is oscillating at the natural shedding frequency, whereas the drag coefficiency is varying at twice the natural shedding frequency like the Nusselt number.

In comparison with the convective heat transfer from a stationary cylinder, an increased time-averaged Nusselt number was predicted with the lock-on oscillation at $S_c = 0.192$ and $A/D = 0.14$, as shown in Fig. 7(b). The time-averaged drag coefficient and the amplitude of the oscillation of the life coefficient are both elevated appreciably by the oscillation of the cylinder.

Detailed information for the effects of lock-on on the heat transfer behavior of an oscillating cylinder is presented in Fig. 8. The dependence of the time-averaged overall Nusselt number, in the form of $\overline{Nu}/\overline{Nu}_0$, on the dimensionless frequency of the oscillation of the cylinder at $Re = 200$, $Pr = 0.71$, and $A/D = 0.14$ is examined. The experimental data presented by Cheng, Chen and Aung [30] are also given in this figure for comparison. Both the predicted and the experimental data show that it is only when the cylinder oscillates at a frequency close to the natural shedding frequency, that the Nusselt number is appreciably increased. Outside this regime, the heat transfer is almost unaffected by the oscillation. This implies that the lock-on effect is the dominant factor that enhances the heat transfer for laminar flows. The peak value in the lock-on regime ($\overline{Nu}_{PL}$) is found to be a function of the Reynolds number as well as the amplitude of oscillation of the cylinder.

Based on the numerical results obtained in this study, a correlation formula expressing the dependence of $\overline{Nu}_{PL}$ on these physical parameters is obtained as

$$\overline{Nu}_{PL} = 0.68 Re^{0.485} Pr^{0.4} [1 + 0.0944(A/D) + 0.118(A/D)^2] \quad (15)$$

which is valid for $80 \leqslant Re \leqslant 300$, $0 \leqslant A/D \leqslant 0.7$, and $0.71 \leqslant Pr \leqslant 7$ with 5% error compared with the numerical solutions. Table 2 displays the values of $\overline{Nu}_{PL}/\overline{Nu}_0$ at $Re = 200$ predicted by the numerical calculations and those derived from equation (15), for various oscillation amplitudes. Meanwhile, the exper-

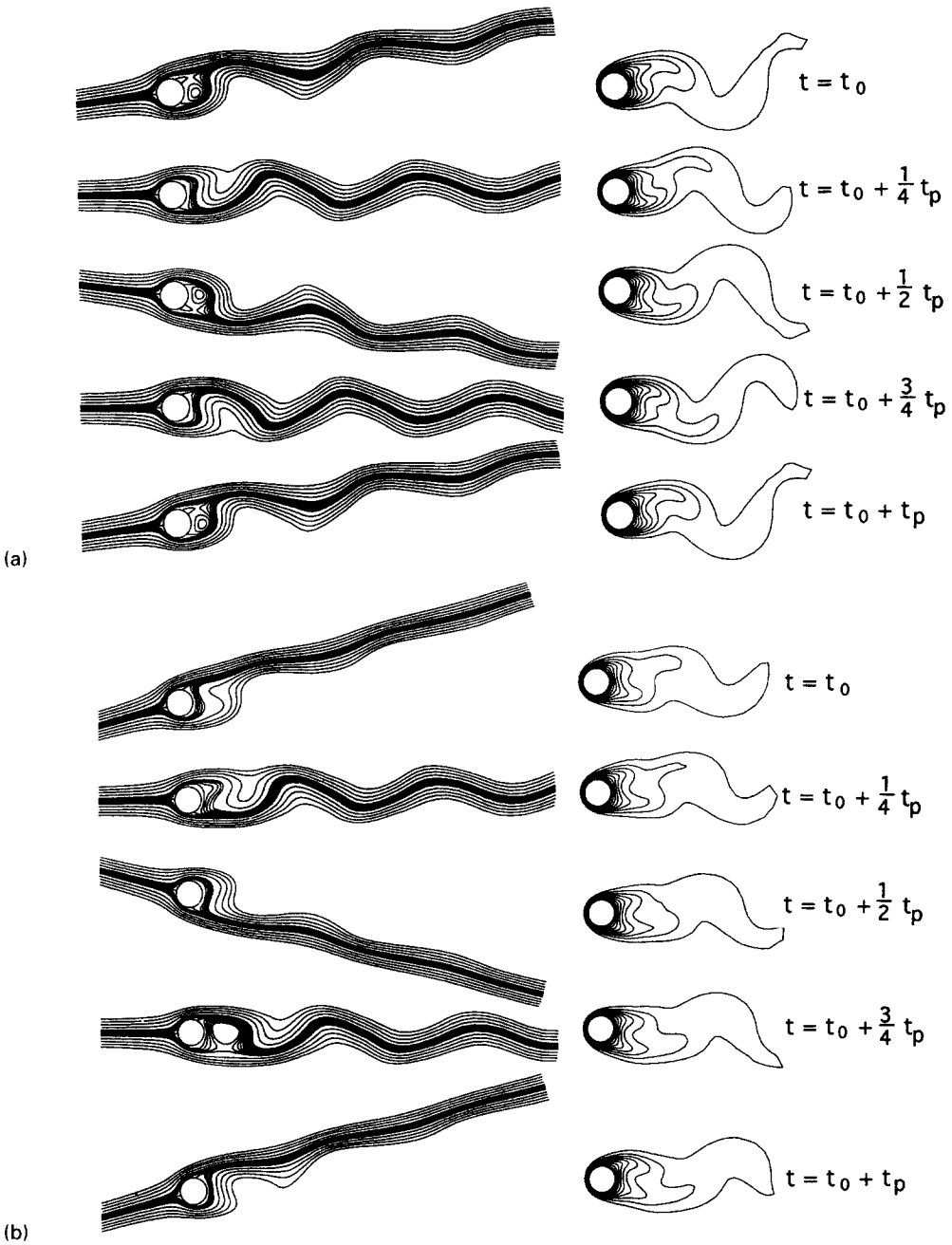

Fig. 5. Unsteady velocity and temperature fields for lock-on and unlock-on flows at $Re = 80$, $Pr = 0.71$, and $A/D = 0.14$ (a) lock-on flow, at $S_c = 0.155$ ($t_p = 6.45$); (b) unlock-on flow, at $S_c = 0.3$ ($t_p = 3.33$).

imental data presented by Cheng, Chen and Aung [30] and the numerical solutions of Karanth, Rankin and Sridhar [31], at this Reynolds number, are also gathered here to integrate the existing information. Results show that the lock-on effect on heat transfer is not significant at low amplitude; however, as the amplitude of the oscillation of the cylinder is elevated, the heat transfer enhancement becomes appreciable. Approximately a 13% increase in heat transfer may be achieved due to the lock-on effects when A/D is elevated to 0.7. All the data from various sources display a similar amplitude-dependence trend. The values calculated from equation (15) basically agree with the experimental data reported by Cheng, Chen and Aung [30]. However, it is noted that more experimental data concerning the turbulence effects resulting from the oscillation of the cylinder at higher Reynolds number or larger amplitude are still needed.

Accompanying the enhancement in heat transfer due to the oscillation effect, an increase in the drag

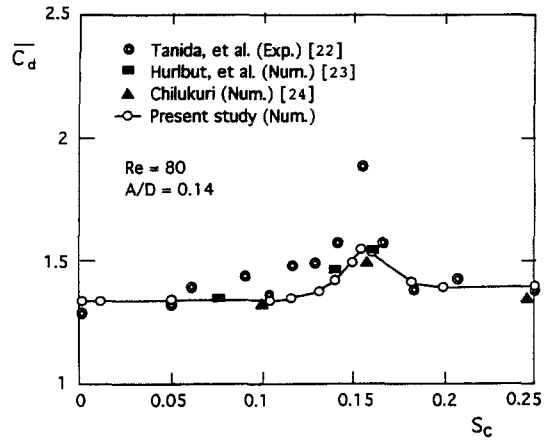

Fig. 6. Lock-on effects on time-averaged drag coefficient at $Re = 80$ and $A/D = 0.14$, compared with existing studies [22–24].

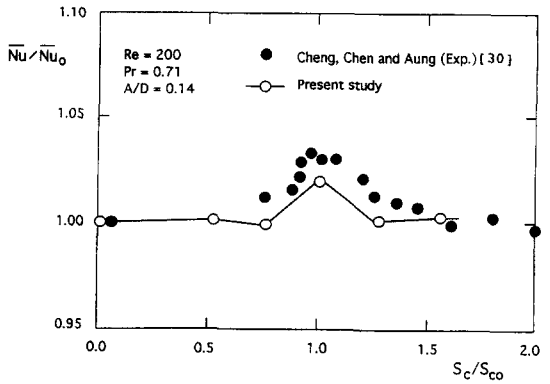

Fig. 8. Lock-on effects on time-averaged overall Nusselt number at $Re = 200$, $Pr = 0.71$, and $A/D = 0.14$.

coefficient is expected. Figure 9 shows the influence of A/D on the peak values of the time-averaged drag coefficient ($\overline{C_{dPL}}$) and the Nusselt number ($\overline{Nu}_{PL}$) in the lock-on regime at $Re = 200$ and $Pr = 7.0$. In this figure the value of $\overline{C_{dPL}}$ is varied from 1.312 to 2.08 as A/D is elevated to 0.7.

CONCLUDING REMARKS

The heat transfer characteristics and flow behavior of a cross flow over a transversely oscillating cylinder

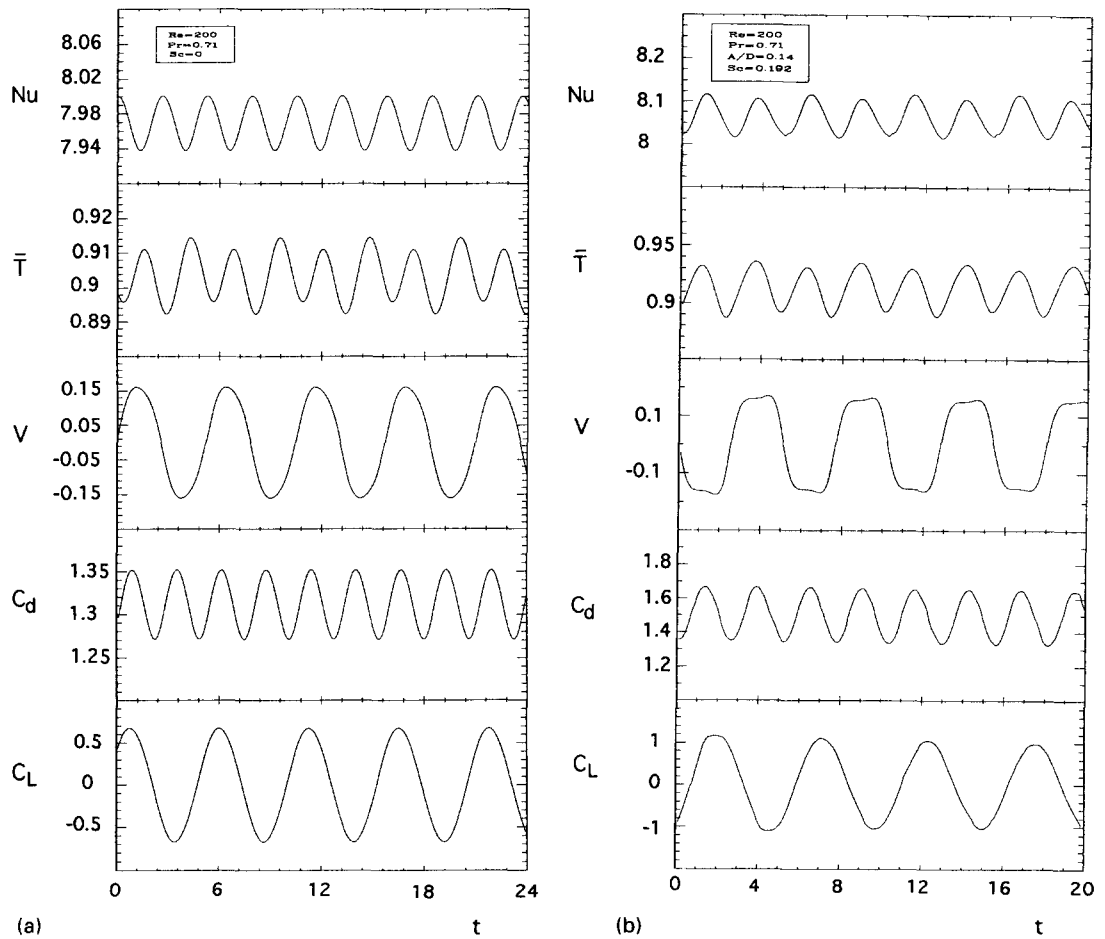

Fig. 7. Time histories of several physical quantities at $Re = 200$ and $Pr = 0.71$ (Nu, C_d and C_L, on cylinder surface; $\bar{T}$ and V, at point $(R, \theta) = (5, 0)$): (a) $S_c = 0$ (stationary cylinder); (b) $S_c = 0.192$, $A/D = 0.14$ (lock-on oscillation).

Table 2. Peak value of time-averaged overall Nusselt number in lock-on regime as a function of dimensionless oscillation amplitude at $Re=200$ and $Pr=0.71$, compared with existing studies [30, 31] and with equation (15).

	$\overline{Nu}_{PL}/\overline{Nu}_0$			
A/D	Ref. [30]	Ref. [31]	Present numerical data	Equation (15)
0	1	1	1	1
0.14	1.03	—	1.016	1.0155
0.2	—	1.016†	—	1.0236
0.3	1.04	—	1.0388	1.0389
0.4	—	1.05†	—	1.0566
0.5	—	—	1.075	1.0767
0.7	—	—	1.125	1.124

† Values taken from Fig. 8 of ref. [31].

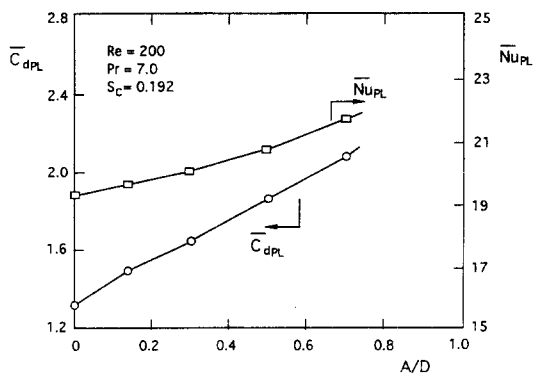

Fig. 9. Peak values of time-averaged drag coefficient and overall Nusselt number in lock-on regime as functions of dimensionless oscillation amplitude, at $Re = 80$ and $Pr = 0.71$.

are investigated. Lock-on phenomenon has been predicted numerically and its influence on the heat transfer performance of the cylinder is evaluated. Numerical solutions of the unsteady flow and temperature fields, time-averaged overall Nusselt number, and time-averaged drag lift coefficients under various physical and oscillation parameters are presented. The parameter ranges considered in this study are $0 \leqslant Re \leqslant 300$, $0 \leqslant S_c \leqslant 0.3$, and $0 \leqslant A/D \leqslant 0.7$. Prandtl numbers assigned are 0.71 and 7.0 pertaining to different fluids. The numerical predictions have been compared with the existing experimental and numerical information for the flow over a stationary or an oscillating cylinder, and good agreement has been found.

Lock-on resonance can be predicted and observed by the numerical calculation when the cylinder oscillates at a frequency close to the natural shedding frequency. Appreciable increase in the Nusselt number may result from the oscillation particularly in this lock-on regime. The peak value of the time-averaged overall Nusselt number in the lock-on regime ($\overline{Nu}_{PL}$) is found to be a function of the Reynolds number as well as the dimensionless amplitude of the oscillation of the cylinder. Based on the present numerical results, a correlation formula expressing the dependence of $\overline{Nu}_{PL}$ on these physical parameters has been obtained.

For the particular case at $Re = 200$ and $Pr = 0.71$, an approximate 13% increase in heat transfer may be achieved due to the lock-on effects when A/D is elevated to 0.7. However, accompanying the enhancement in heat transfer due to cylinder oscillation, an increase in the drag coefficient from 1.312 to 2.08 is also found.

The numerical predictions of the lock-on effect on the heat transfer basically agrees with the experimental data provided by Cheng, Chen and Aung [30]. However, more experimental studies concerning the turbulence effect resulting from the oscillation of the cylinder are still needed.

Acknowledgement—The financial support of this work by the National Science Council, Republic of China, under Grant no. NSC 85-2212-E-036-004, is gratefully acknowledged.

REFERENCES

1. Tritton, D. J., Experiments on the flow past a circular cylinder at low Reynolds number. *Journal of Fluid Mechanics*, 1959, **6**, 547–567.
2. Wille, R., Karman vortex streets. In *Advanced Applied Mechanics*, Vol. 6. Academic Press, New York, 1960, p. 273.
3. Thoman, D. C. and Szewczyk, A. A., Time dependent viscous flow over a circular cylinder. *Physics of Fluids*, 1969. **12**, 79–86.
4. Jordan, S. K. and Fromm, J. E., Oscillatory drag, lift and torque on a circular cylinder in a uniform flow. *Physics of Fluids*, 1972, **15**, 371–376.
5. Lin, C. L., Pepper, D. W. and Lee, S. C., Numerical methods for separated flow solutions around a circular cylinder. *AIAA Journal*, 1976, **14**, 900–907.
6. Martinez, G., Caracteristiques dynamiques et thermiques de l'ecoulement autour d'un cylindre circulaire a nombres de Reynolds moderes. Ph.D. Thesis, L'Institute National Polytechnique de Toulouse, France, 1979.
7. Borthwick, A., Comparison between two finite-difference schemes for computing the flow around a cylinder. *International Journal for Numerical Methods in Fluids*, 1986. **6**, 275–290.
8. Braza, M., Chassaing, P. and Minh, H. H., Numerical study and physical analysis of the pressure and velocity fields in the near wakes of a circular cylinder. *Journal of Fluid Mechanics*, 1986, **165**, 79–130.
9. Lecointe, Y. and Piquet, J., Flow structure in the wake of an oscillating cylinder. *Journal of Fluids Engineering*, 1989, **111**, 139–148.
10. Sa, J. Y. and Chang, K. S., Shedding patterns of the near-wake vortices behind a circular cylinder. *International Journal for Numerical Method in Fluids*, 1991, **12**, 463–474.
11. Dimopoulos, H. G. and Hanratty, T., Velocity gradients at the wall for flow around a cylinder for Reynolds numbers between 60 and 360. *Journal of Fluid Mechanics*, 1968, **33**, 303–311.
12. Eckert, E. R. G. and Soehngen, E., Distribution of heat-transfer coefficients around circular cylinder in crossflow at Reynolds numbers from 20 to 500. *Transactions of the ASME*, 1952, **74**, 343–347.
13. Karniadakis, G. E., Numerical simulation of forced convection heat transfer from a cylinder in crossflow. *International Journal of Heat and Mass Transfer*, 1988, **31**, 107–118.

14. Kramers, H. A., Heat transfer from sphere to flowing media. *Physics*, 1946, **12,** 61–80.
15. McAdams, W. H., *Heat Transmission*, 3rd edn. McGraw-Hill, New York, 1954.
16. Tsubouchi, T. and Masuda, A. H., Report No. 191, Institute of High Speed Mechanics, Tohoku University, Japan, 1966.
17. Jain, P. C. and Goel, B. S., A numerical study of unsteady laminar forced convection from a circular cylinder. *Journal of Heat Transfer*, 1976, **98,** 303–307.
18. Yang, Y. T., Chen, C. K. and Wu, S. R., Transient laminar forced convection from a circular cylinder using a body-fitted coordinate system. *Journal of Thermophysics*, 1992, **6,** 184–188.
19. Hudson, J. D., Dennis, S. C. R. and Smith, N., Steady laminar forced convection from a circular cylinder at low Reynolds numbers. *Physics of Fluids*, 1968, **11,** 933–939.
20. Badr, H. M., A theoretical study of laminar mixed convection from a horizontal cylinder in a cross stream. *International Journal of Heat and Mass Transfer*, 1983, **26,** 639–653.
21. Chen, C. H. and Weng, F. B., Heat transfer for incompressible and compressible fluid flows over a heated cylinder. *Numerical Heat Transfer*, 1990, **18,** 325–342.
22. Tanida, Y., Okajima, A. and Watanabe, Y., Stability of a circular cylinder oscillating in uniform flow or in a wake. *Journal of Fluid Mechanics*, 1973, **61,** 769–784.
23. Hurlbut, S. E., Spaulding, M. L. and White, F. M., Numerical solution for laminar two dimensional flow about a cylinder oscillating in a uniform stream. *Journal of Fluids Engineering*, 1982, **104,** 214–222.
24. Chilukuri, R., Incompressible laminar flow past a transversely vibrating cylinder. *Journal of Fluids Engineering*, 1987, **109,** 166–171.
25. Griffin, O. M. and Hall, M. S., Review-vortex shedding lock-on and flow control in bluff body wakes. *Journal of Fluids Engineering*, 1991, **113,** 526–537.
26. Kezios, S. P. and Prasanna, K. V., Effect of vibration on heat transfer from a cylinder in normal flow. ASME Paper no. 66-WA/HT-43, 1966.
27. Saxena, U. C. and Laird, A. D. K., Heat transfer from a cylinder oscillating in a cross-flow. *Journal of Heat Transfer*, 1978, **100,** 684–689.
28. Sreenivasan, K. and Ramachandran, A., Effect of vibration on heat transfer from a horizontal cylinder to a normal air stream. *International Journal of Heat and Mass Transfer*, 1961, **3,** 60–67.
29. Leung, C. T., Ko, N. W. M. and Ma, K. H., Heat transfer from a vibrating cylinder. *Journal of Sound and Vibration*, 1981, **75,** 581–582.
30. Cheng, C. H., Chen, H. N. and Aung, W., Experimental study on the effect of transverse oscillation on convection heat transfer from a circular cylinder. In *Advances in Enhanced Heat Transfer*, ASME HTD-Vol. 287, 1994, pp. 25–34.
31. Karanth, D., Rankin, G. W. and Sridhar, K., A finite difference calculation of forced convection heat transfer from an oscillating cylinder. *International Journal of Heat and Mass Transfer*, 1994, **37,** 1619–1630.
32. Hirt, C. W., Nichols, B. D. and Romero, N. C., SOLA—a numerical solution algorithm for transient fluid flows. Los Alamos Scientific Laboratory report no. LA4370, 1970.
33. Cheng, C. H., Luy, C. D. and Huang, W. H., Buoyancy effect on the heat convection in vertical channels with fin array at low Reynolds numbers. *International Journal of Heat and Mass Transfer*, 1992, **35,** 2643–2653.
34. Patankar, S. V., *Numerical Heat Transfer and Fluid Flow*. Hemisphere, Washington, DC, 1980.